CT Fluoroscopy-Guided Robotically-Assisted Lung Biopsy

Sheng Xu*[a], Gabor Fichtinger[a], Russell H. Taylor[a], Filip Banovac[b], and Kevin Cleary[b]

[a]Engineering Research Center, Johns Hopkins University, Baltimore, MD 21218, MD USA;
[b]Imaging Science and Information Systems (ISIS) Center, Department of Radiology, Georgetown University Medical Center, Washington, DC 20007 USA

ABSTRACT

Lung biopsy is a common interventional radiology procedure. One of the difficulties in performing the lung biopsy is that lesions move with respiration. This paper presents a new robotically assisted lung biopsy system for CT fluoroscopy that can automatically compensate for the respiratory motion during the intervention. The system consists of a needle placement robot to hold the needle on the CT scan plane, a radiolucent Z-frame for registration of the CT and robot coordinate systems, and a frame grabber to obtain the CT fluoroscopy image in real-time. The CT fluoroscopy images are used to noninvasively track the motion of a pulmonary lesion in real-time. The position of the lesion in the images is automatically determined by the image processing software and the motion of the robot is controlled to compensate for the lesion motion. The system was validated under CT fluoroscopy using a respiratory motion simulator. A swine study was also done to show the feasibility of the technique in a respiring animal.

Keywords: lung biopsy, motion tracking, real-time image processing, medical robotics

1. INTRODUCTION

1.1 Clinical Significance

Lung biopsy is a common interventional radiology procedure. The purpose of the procedure is to obtain a tissue sample from a suspicious lesion in the lung. This tissue sample is then analyzed by a pathologist to determine if cancer is present. As lung cancer screening becomes more prevalent, an increasing number of suspicious lesions will be found, and more lung biopsies will be required[1].

One of the difficulties in lung biopsy is that lesions move with respiration, which can make it difficult to locate lesions and accurately perform the biopsy. CT fluoroscopy (CTF) combines the advantages of both CT and fluoroscopy in that moving lesions in internal organs can be viewed in nearly real-time, allowing compensation for respiratory motion during the intervention. It is also possible to see the needle's interaction with the target lesions under CTF, resulting in improved success rate of the percutaneous biopsy[2] (CTF 93.7% vs. CT 88.2%). Additionally, CTF decreases procedure time by at least a factor of 2 compared with conventional CT guided procedures[3].

Currently, lung biopsy is performed freehand. Based on preoperative image data, the physician identifies the skin entry point and the lesion, thus defining the desired needle trajectory. The physician then aligns the needle by hand and partially inserts it towards the lesion. The physician proceeds with further insertion of the needle, checking the position of the needle by re-scanning as necessary. The main problem with freehand biopsy is that the physician's accuracy is limited when initially lining up the needle and then staying on course throughout the procedure. Additionally, when the

* sheng@cs.jhu.edu; phone 1 301 594-2073; fax 1 301 480-1932

Medical Imaging 2006: Visualization, Image-Guided Procedures, and Display, edited by Kevin R. Cleary, Robert L. Galloway, Jr., Proc. of SPIE Vol. 6141, 61411L, (2006)
1605-7422/06/$15 · doi: 10.1117/12.652882

physician releases the needle, the needle can drift or tilt away from the desired path. In response to these problems, we propose integrating CTF imaging with a medical robot for precise placement of the needle.

1.2 Prior Technical Developments

For robotically assisted needle placement, one important concept is the remote center of motion (RCM) which provides rotational motion around a fixed fulcrum point in space. Stoianovici developed a two degrees-of-freedom (DOF) RCM robot with a radiolucent needle driver for percutaneous renal access under fluoroscopic guidance[4]. Taylor adapted the RCM module for microsurgical augmentation[5].

In addition to the hardware developments, many robotic systems have been integrated with guiding imaging modalities. Hong[6] presented an ultrasound-driven needle-insertion robot for percutaneous cholecystostomy. Loser[7] presented a system for needle insertion guided by visual servoing in a CTF scanner. Bascle presented an approach for needle placement under X-ray fluoroscopy[8]. Susil[9] developed a registration method using a Z-frame for needle insertion inside a CT scanner.

2. METHOD

2.1 System Components

As shown in figure 1, the main system components include a CTF scanner, a needle insertion robot with an associated control computer, a Z-frame, a frame grabber, and an image processing computer.

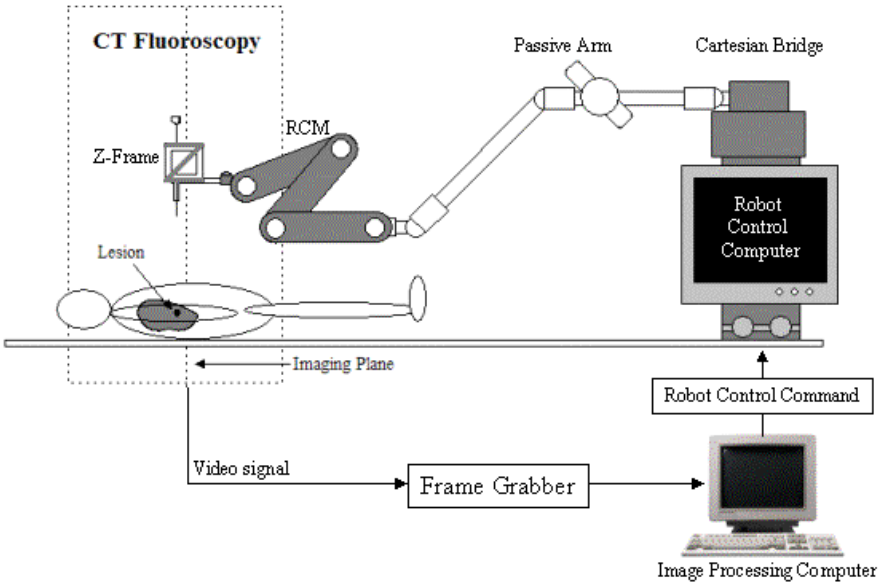

Figure 1: System components

The CTF scanner is a Siemens Somatom Volume Zoom. The maximum frequency of the CTF scan is approximately 6Hz. The needle placement robot was developed by the Urology Robotics Group at Johns Hopkins Medical Institutions[10]. It includes a 3-Degrees-Of-Freedom (DOF) Cartesian motion stage mounted on the CT table so that the robot will move with the CT table. The Cartesian stage is connected to a 7-DOF adjustable unencoded passive arm, used for gross positioning of the needle drive stage. The rotation stage is a 2-DOF RCM. The needle drive stage is a 1-DOF friction transmission with a radiolucent end-effector[8] integrated with a Z-frame for registration of the robot and CT[9].

During the lung biopsy intervention, CTF images are obtained as needed to position the needle. The real-time display from the CTF monitor is captured using a frame grabber (Accustream 170, Foresight Imaging, Lowell, Massachusetts, USA). The frame grabbed images are processed by an image processing computer to estimate the real-time position of the target lesion. The image processing computer then uses the inverse kinematics of the robot to generate control commands which are sent to the robot through an ethernet cable and TCP/IP connection. The robot then moves accordingly to compensate for the respiratory motion of the patient.

2.2 Clinical Workflow

The envisioned scenario for CTF-guided robotically assisted lung biopsy is as follows:

1. The patient is scanned under breath holding to obtain a 3D preoperative CT volume at the end-of-inspiration.
2. The physician selects the entry and target locations of the biopsy path in the CT volume.
3. The physician starts the CTF scan, allowing the system to track the real-time position of the target lesion.
4. Patient's skin at the entry point is anesthetized with 1% Lidocaine.
5. The robot moves the needle to the entry point, aligns the needle with the path, and inserts the needle into the target lesion based on the motion tracking result.
6. The robot releases the needle.
7. The physician manually inserts the needle under the guidance of the needle holder of the robot.
8. The physician injects the therapeutic agent or takes the biopsy sample.

In order to increase safety, the physician supervises the needle insertion at the robot control computer. The system can be halted at any time by the physician. Before the needle enters the body, the robot can make quick adjustments of the needle pose based on the real-time position of the target lesion. The patient holds their breath during the needle insertion to ensure accurate targeting and to avoid potential needle bending. Once the needle is in the lesion, the robot should release the needle so that the patient can breathe again and the needle can move freely with respiration. The current needle driver does not allow us to release the needle, but a new version of the needle driver is being designed to include this feature.

2.3 Three Dimensional Motion Tracking of Pulmonary Lesions

In lung biopsy, the position of the target lesion may vary due to intrinsic causes such as respiratory motion or extrinsic reasons such as interactions between the tissue and a surgical tool. The positioning information of the lesion obtained from the preoperative CT scan may not be correct during the intervention. Therefore, it is necessary to track the lesion's motion in 3D space. CTF can be used for motion tracking in that it allows the tissue inside the imaging plane to be viewed in real-time. In order to estimate both in-plane and out-of-plane motion of the lesion, the patient needs to be positioned carefully on the CT table so that the lesion moves within a certain distance from the imaging plane during respiration. This is feasible because respiratory motion is limited to a few centimeters, allowing the off-plane motion of the target lesion to be estimated using the lung tissue inside the imaging plane. The motion-tracking algorithm is based on minimizing the Zero-mean Sum of Squared Differences (ZSSD) between a reference CTF image region and a corresponding region in the preoperative CT volume. The relative position between the target and the reference CTF region can be obtained in the preoperative CT volume, which can be used to estimate the lesion's real-time position with respect to the CTF imaging plane. The details of this tracking algorithm are described in [11].

2.4 Registrations and Coordinate Transformations

The goal of this system is to insert the needle into the target. The real-time transformation between the needle and the target can be calculated as following:

$$F_{Target}^{Needle} = F_{Z-frame}^{Needle} \bullet F_{CT}^{Z-frame} \bullet F_{CTF}^{CT} \bullet F_{Target}^{CTF} \quad (1)$$

where F_A^B represents a 4x4 homogeneous transformation matrix from the source coordinate system A to the target coordinate system B.

From the right of to the left of equation (1), F_{Target}^{CTF} contains the real-time position of the lesion with respect to the CTF imaging plane, obtained from the motion-tracking algorithm[11]; F_{CTF}^{CT} consists of the fixed translation from the origin of the frame grabbed CTF image to the origin of the preoperative CT volume, obtained from a translation registration (3-DOF) of a static rigid body in both images. Since the Z-frame is attached to the robot, $F_{CT}^{Z-frame}$ is a fixed transformation from the CT space to the robot space. The Z-frame contains three "Z"s that are formed by seven radiolucent fiducial rods located at known positions. As shown in figure 2, a single cross sectional CT image allows the rigid-body transformation between the CT and the Z-frame to be determined[7]. $F_{Z-frame}^{Needle}$ is the fixed transformation from the Z-frame to the needle space.

(b) A CT slice of Z-frame (c) Registered Z-frame

Figure 2: Registration of Z-frame to CT

Since the RCM and Cartesian stages are connected by a passive arm, they need to be registered to the CT space separately. The RCM is registered through the attached Z-frame. Since the Cartesian stage is rigidly attached to the CT table using a curved mount and nylon straps, (figure 3.a), it is considered to be aligned with coordinate system of the CT scanner. This assumption is reasonable because respiratory motion is limited to a few centimeters. In such a small motion range, the motion error of the robot introduced by any misalignment of the Cartesian stage and CT table is negligible. To move the needle from its current needle position to the target position, the motion of the robot can be calculated from F_{Target}^{Needle} and the inverse kinematics of the robot.

2.5 Compensation for the Motion of Target Lesion

To compensate for the motion of the target lesion, a control loop is executed in the software. The needle is retracted from the RCM center to avoid any potential collision with the patient during the tracking. The following steps are executed inside the loop:

1. Process the CTF image to obtain the real-time position of the target lesion.
2. Update the biopsy path using the result of motion tracking.
3. Apply the inverse kinematics of the robot to update the needle pose according to the new path.

This is a typical control strategy that combines the visual sensing and manipulation in an open loop fashion, "looking then moving"[5], in which the CTF is the camera or the eye fixed on the ground. As a prototypical system, the skin entry point is currently assumed to be independent from respiration. Therefore, only the needle orientation needs to be updated to compensate for respiratory motion. In reality, the motion of the skin entry point may not be negligible. Although both the hardware and software of the system are capable of compensating for the lesion's motion in nearly real-time, for safety reasons, we envision that in any clinical use the needle will be manually inserted by the physician after the needle

is aligned. Particularly in lung biopsy, automatic needle insertion using robot may increase the chance of pneumothorax. Therefore, the patient is asked to hold his or her breath during the insertion to avoid potential needle bending. The needle's position is automatically adjusted only before it enters the patient.

3. EXPERIMENTS AND RESULTS

To test the system's performance, both phantom and swine studies were conducted at Georgetown University Medical Center on a Siemens Volume Zoom CT/CTF scanner. The frame rate of the CTF scans was 6 Hz.

3.1 Phantom Study

The accuracy of the system was evaluated in a phantom study using a respiratory motion simulator. Since the motion-tracking algorithm relies heavily on the texture of the lung, we developed a lung phantom with similar texture information. The phantom was made from seashells and rice packaged in a tennis ball container as shown in figure 3.b. The phantom was mounted on a 3D translational stage which held the phantom on the CTF scan plane and could be computer controlled to simulate any motion pattern. This 3D translational stage was originally developed to serve as a respiratory motion simulator during CyberKnife radiotherapy motion compensation experiments[12].

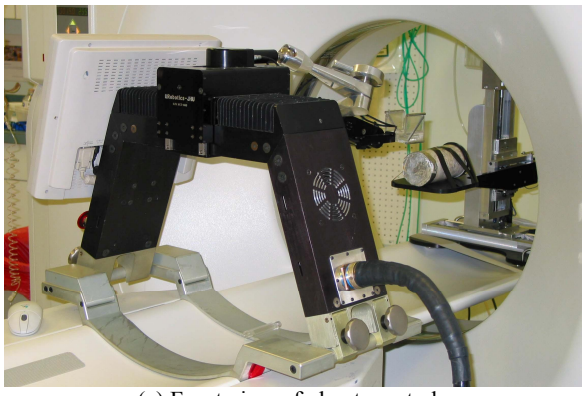

(a) Front view of phantom study

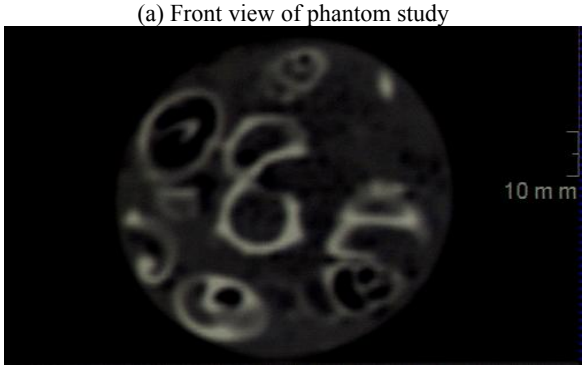

(b) CT image of lung phantom

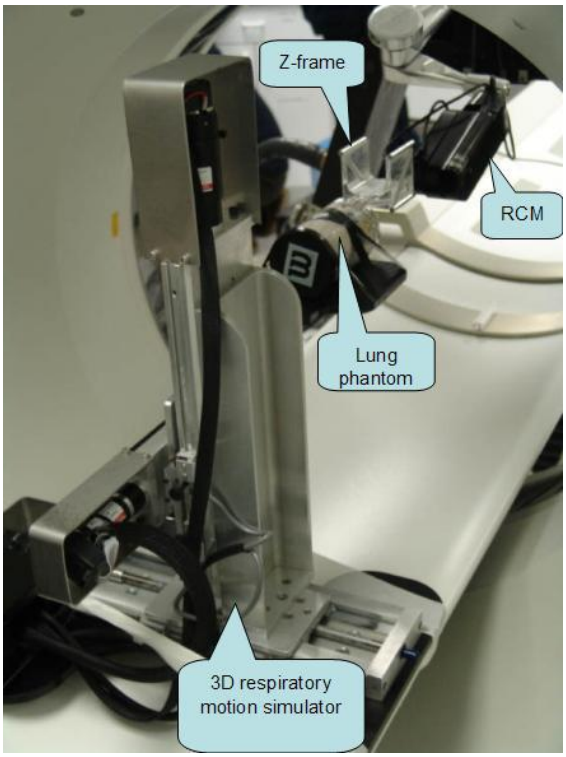

(c) Back view of phantom study

Figure 3: Phantom study

Before the experiments, the motion simulator was manually aligned with the CT table. Several 1 mm fiducials were attached to the surface of the phantom. The phantom was CT scanned with a 1 mm slice thickness and 0.74 mm pixel size. A fiducial on the phantom surface was selected as the needle target. The needle entry point was selected to be in the air above. After the system was initialized, the phantom was moved by the respiratory motion simulator from its original position to some other known position. A CTF image at the new position was obtained. The frame grabbed CTF image was processed to obtain the position of the target lesion. The robot then moved, aligned and drove the needle to the target. The difference between the target and the final robot position was measured to obtain the accuracy of the system.

To measure the system error, the encoders of the robot were used as a precision measuring device. The robot was manually moved using its translational stage until the needle tip touched the target fiducial. The amount the robot had to be moved was recorded as the system error as shown in Table 1. The tracking error was also estimated in this study by comparing the motion amplitude detected by the tracking algorithm to the programmed amplitude (Table 1).

Table 1: Experimental Results

Parameter Measured	Number of Trials	Average Error	Variance of Error
System error	10	1.7 mm	0.5 mm
Tracking error	10	0.4 mm	0.3 mm

Although the motion in the above study was not continuous, comparable results were observed in another study under continuous phantom motion. As shown in figure 4, the respiratory motion simulator was commanded to move in sinusoid curves along the three principal axels simultaneously. Since no synchronization was used in the study, the results of motion tracking were fit to the ground truth of the programmed motion.

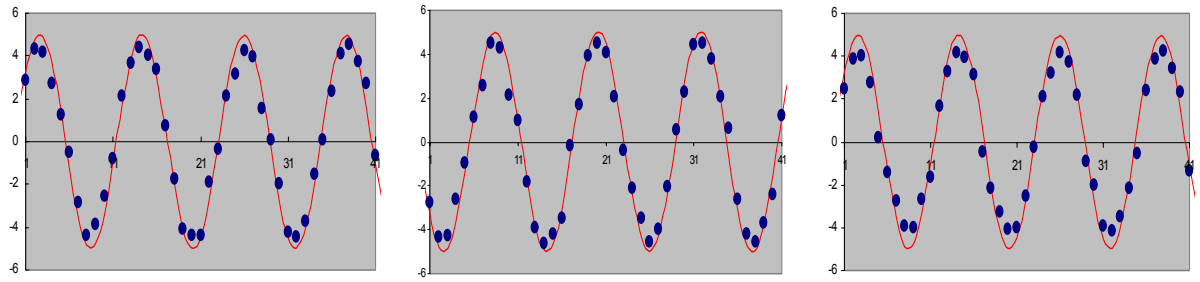

(a) Left-Right Motion (b) Anterior-Posterior Motion (c) Superior-Inferior Motion

Figure 4: Results (blue dots) of motion tracking in mm. Red lines are the ground truth.

3.2 Swine Study

The system was also tested in animal studies under an approved animal care protocol, with endotracheal intubation and under general anesthesia. A 3D CT scan was taken with the ventilator held in end respiratory phase of the tidal volume breathing cycle. To avoid the risk of inducing a pneumothorax and compromising the animal, no fiducial markers was implanted in the lung. Instead, an anatomical location of the lung was identified in the CT volume as the target point. During the treatment, the swine was mechanically ventilated. The CTF images were used to track the motion of the target point. At a certain respiratory phase, the ventilator was stopped to simulate the breath holding of the swine. The end-effector was aligned based on the motion-tracking algorithm; then, the needle was pushed into the lung by hand.

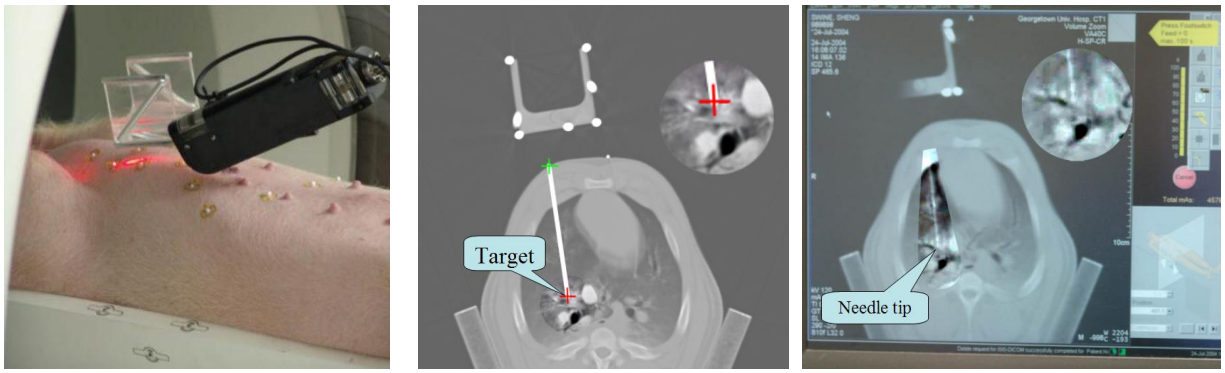

(a) Swine in CTF (b) Planned needle path (c) Actual needle path

Figure 5: Swine study

Figure 5.a shows one of the animal studies. Figure 5.b shows the planned path in the preoperative CT volume, and figure 5.c shows the actual needle path. Although there was no numerical ground truth to validate the needle insertion, good correspondence between the two paths was observed from the images, meaning that the system was able to accurately align the needle. While this is just a preliminary result, this gives us confidence that the system can track the respiratory motion of the lung, and further animal studies are planned.

4. CONCLUSION AND DISCUSSION

In this paper, we presented the feasibility of using an image-guided surgical robot to assist lung biopsy. The system integrates a real-time non-invasive tracking algorithm to detect the motion of a pulmonary lesion. An open-loop control is used to automatically compensate for the target's motion. Initial experimental results showed that the biopsy system worked well with a respiratory motion simulator and had reasonable performance in a swine study. There are currently no other published systems for noninvasive real-time motion compensation of pulmonary tumors.

While the experiments validated the overall system concept, several weaknesses were identified that need to be addressed. First, we did not achieve a sufficient working volume, due to interference among the relatively large Z-frame, the RCM and the patient. We could not reach all clinically significant locations in the phantom and swine studies, especially considering oblique angles. The robot's passive arm had to be very carefully manipulated to ensure that not only the Z-frame stayed in the CTF filed of view but also the RCM didn't collide on the patient. Therefore, the RCM and the Z-frame need to be redesigned to allow for more clearance for the robot during needle placement. Second, the robot was rather sluggish in following the target's motion. We must note, however, that typical surgical robots are not supposed to perform quick motions, in order to reduce potential injury to the patient. Finally, the motion-tracking algorithm is only accurate when the target is close to the CTF imaging plane[13]. The algorithm is not robust for lung regions that don't have enough texture.

In addition to improving the tracking algorithm's robustness and accuracy, future work will include developing a new needle driver so that the needle can be automatically released from the needle driver once the needle has reached the desired position[14]. As a safety feature, it would also be desirable to integrate force sensing in the needle driver so that the needle could be released when abrupt motion of the patient is detected by processing real-time CTF image. Finally, the real-time needle position can also be obtained by tracking the Z-frame in the CTF image. Using a method such as visual servoing, the needle position can be automatically detected and used to adjust the needle's pose with respect to the target lesion. The control loop of the system can then be closed, which is called "dynamic look-and-move"[7].

ACKNOWLEDGEMENT

This work was primarily supported by U.S. Army grants W81XWH-04-1-0078 and DAMD17-99-1-9022 and National Cancer Institute (NIH) grant 1 R21 CA094274-01A1. Research infrastructure was also provided by the National Science Foundation under ERC cooperative agreement EEC9731478. The robot was designed and constructed by Dan Stoianovici, PhD, of the URobotics Laboratory at the Johns Hopkins Medical Institutions. Thanks are due to Emmaneul Varghese, Ziv Yaniv, and David Lindisch of Georgetown University for their help with the experiments.

REFERENCES

1. K. Cleary, M. Mulcahy, R. Piyasena, T. Zhou, S. Dieterich, S. Xu, K. Wong, "Organ motion due to respiration: the state-of-the-art and applications in interventional radiology and radiation oncology", Proc. *SPIE: Visualization, Image-Guided Procedures and Display, Medical Imaging*, vol. 5744, pp. 53-9, 2005.

2. D. Gianfelice, L. Lepanto, P. Perreault, C. Chartrand-Lefebvre, and P. C. Milette, "Value of CT fluoroscopy for percutaneous biopsy procedures," J Vasc Interv Radiol, vol. **11**, pp. 879-84, 2000.
3. E. M. Law, A. F. Little, and J. C. Salanitri, "Non-vascular intervention with real-time CT fluoroscopy," Australas Radiol, vol. **45**, pp. 109-12, 2001.
4. D. Stoianovici, L. L. Whitcomb, J. H. Anderson, R. H. Taylor, and L. R. Kavoussi, "A Modular Surgical Robotic System for Image-Guided Percutaneous Procedures," *MICCAI*: *Lecture Notes in Computer Science*, vol. 1496, pp. 404-410, Springer-Verlag, 1998.
5. R. H. Taylor, P. Jensen, L. Whitcomb, A. Barnes, R. Kumar, D. Stoianovici, P. Gupta, Z. Wang, E. deJuan, and L. Kavoussi, "A Steady-Hand Robotic System for Microsurgical Augmentation," International Journal of Robotics Research, vol. **18**, no. 12, pp. 1201-1210, Dec. 1999.
6. J. Hong, T. Dohi, M. Hashizume, K. Konishi, N. Hata: "An Ultrasound-driven Needle Insertion Robot for Percutaneous Cholecystostomy" , Physics in Medicine and Biology, Vol.49, No.**3**, pp.441-455, 2004.
7. M. Loser and N. Navab, "A new robotic system for visually controlled percutaneous interventions under CT Fluoroscopy," *MICCAI*: *Lecture Notes in Computer Science*, vol. 1935, pp 887-896, Springer Verlag, 2000.
8. B. Bascle, N. Navab, M. Loser, B. Geiger, R. Taylor, "Needle placement under X-ray fluoroscopy using perspectiveinvariants", Mathematical Methods in Biomedical Image Analysis, pp. 46-53, 2000.
9. R. C. Susil, J. H. Anderson, R. H. Taylor, "A Single Image Registration Method for CT-Guided Interventions," *MICCAI*: *Lecture Notes in Computer Science*, vol. 1679, pp. 798-808, Springer-Verlag, 1999.
10. D. Stoianovici, K. Cleary, A. Patriciu, D. Mazilu, A. Stanimir, N. Craciunoiu, V. Watson, and L. R. Kavoussi, "AcuBot: a robot for radiological interventions," IEEE Transactions on Robotics and Automation, vol. **19**, pp. 927-930, 2003.
11. S. Xu, G. Fichtinger, R. H. Taylor, and K. R. Cleary, "3D motion tracking of pulmonary lesions using CT fluoroscopy images for robotically assisted lung biopsy," Proc. *SPIE: Visualization, Image-Guided Procedures and Display, Medical Imaging*, vol. 5367, pp. 394-402, 2004.
12. T. Zhou, J. Tang, S. Dieterich, and K. Cleary, "A robotic 3-D motion simulator for enhanced accuracy in CyberKnife stereotactic radiosurgery," *Computer Aided Radiology and Surgery (CARS)*, pp. 323-328, Elsevier, 2004.
13. S. Xu, G. Fichtinger, Lindisch D, K. Cleary, "Validation of 3D Motion Tracking of Pulmonary Lesions for Image-Guided Lung Biopsy," Proc. *SPIE: Visualization, Image-Guided Procedures and Display, Medical Imaging*, Vol. 5744, pp. 60-68, 2005.
14. I. Iordachita, R. Wiard, G. Fichtinger, I. Sakuma, and D. Stoianovici, "Controllable motorized devices for accurate percutaneous needle placement in soft tissue target," *the 11th World Congress in Mechanisms and Machine Science*, pp. 82-86, 2004.